J Appl Electrochem (2011) 41:551–559
DOI 10.1007/s10800-011-0261-8

ORIGINAL PAPER

Surface modification effects of $[Li,La]TiO_3$ on the electrochemical performance of $Li[Ni_{0.35}Co_{0.3}Mn_{0.35}]O_2$ cathode material for lithium–ion batteries

Kwang Hee Jung · Ho-Gi Kim · Kwang Man Kim · Yong Joon Park

Received: 12 March 2010 / Accepted: 13 February 2011 / Published online: 26 February 2011

Abstract Surface modification of $Li[Ni_{0.35}Co_{0.3}Mn_{0.35}]O_2$ as a cathode material of lithium–ion batteries was carried out by hydrothermal treatment using lithium lanthanum titanate ($[Li,La]TiO_3$). The modified surfaces were analyzed by morphology observation using transmission electron microscopy and by element investigation using X-ray photoelectron spectroscopy. It was thereupon found that the $[Li,La]TiO_3$-coated layer formed by the surface modification played a definitive role in suppressing the solid electrolyte interface during repeated charge and discharge cycles. In addition, the thermal stability was enhanced by coated layer, resulting in an increase of the onset temperature to occur an exothermic reaction during thermal runaway.

Keywords Surface coating · Lithium lanthanum titanate · Cathode · Lithium–ion batteries

1 Introduction

Layered $LiCoO_2$ was one of the earliest developed cathode materials and continues to be a main component for cathodes in rechargeable lithium batteries due to its advantages of easy preparation, high voltage, and good cycle properties. However, since the commercialization of $LiCoO_2$ by SONY in 1991 [1], many researchers have made an effort to find substitutes for this material due to its toxicity and high cost. $Li(Ni,Co,Mn)O_2$ is one of the most promising new cathode materials [2–4]. Choi and Manthiram systemically investigated the electrochemical performance of $Li[Ni_{0.5-y}Mn_{0.5-y}Co_{2y}]O_2$ found that high capacity and good cyclability were obtained when the Co content was $0.33 \leq 2y \geq 0.5$ [4]. As another approach for enhancing the electrochemical properties, Li-rich layered materials have been employed for lithium secondary batteries [5–7]. A wide range of studies of layered cathode compositions has been reported [2–11], and surface modification of electrode materials for lithium batteries has been identified as a promising method for achieving improved electrochemical properties [12–15]. Studies of surface coating of cathode materials with various stable metal oxides or phosphates such as ZrO_2 [16], TiO_2 [17], MgO [18], $AlPO_4$ [19], and $Co_3(PO_4)_2$ [20] have revealed that coating active materials is an effective approach for improving the electrochemical performance. The coating effect correlates highly with the coating material [17, 20, 21]. Therefore, determining the appropriate coating material for obtaining the desired electrochemical performance of a coated cathode material is a crucial factor. In this study, lithium lanthanum titanate was employed as the coating material. This perovskite-type compound has received considerable attention as a solid electrolyte owing to its high lithium ionic conductivity [22–28]. Surface coating results in enhanced properties of the cathode material, because it suppresses the formation of an unwanted surface layer originating from the dissolution of cations (e.g., Co, Ni, and Mn) and/or the attack of HF on

K. H. Jung · H.-G. Kim
Department of Materials Science and Engineering, Korea Advanced Institute of Science and Technology, Daejeon 305-701, South Korea

K. M. Kim
Power Control Device Research Team, Electronics and Telecommunications Research Institute (ETRI), 138 Gajungno, Yusong, Daejon 305-700, South Korea

Y. J. Park (✉)
Department of Advanced Materials Engineering, Kyonggi University, Gyeonggi-do 443-760, South Korea
e-mail: yjpark2006@kyonggi.ac.kr

the electrolyte [15, 29, 30]. However, the coating material is basically a non-conductive material of lithium ions and electrons, and as such it may act as an obstacle to the diffusion of lithium ions. It is expected that a positive electrode coated with lithium lanthanum titanate will have a greater rate capability owing to use of a coating material with high ionic conductivity. Moreover, lithium lanthanum titanate has higher electronic conductivity than other solid electrolytes. While the high electronic conductivity has been a major problem in its application as a solid electrolyte, it is a major advantage for use as a coating material, because a coating layer with high electronic conductivity facilitates electron movement during the charge/discharge process.

In this study, $Li[Ni_{0.35}Co_{0.30}Mn_{0.35}]O_2$, one of a series of $Li[Ni_{0.5-y}Co_{2y}Mn_{0.5-y}]O_2$ (at $2y = 0.3$), was introduced as a cathode material. We fabricated a surface-modified $Li[Ni_{0.35}Co_{0.3}Mn_{0.35}]O_2$ cathode with the novel coating material $[Li,La]TiO_3$ and examined the electrochemical and structural properties of the coated electrodes. The thermal stability was also investigated to shed light on understand the coating effects.

2 Experimental

$Li[Ni_{0.35}Co_{0.3}Mn_{0.35}]O_2$ was prepared by a sucrose combustion method from manganese(II) nitrate hexahydrate ($Mn(NO_3)_2{\cdot}6H_2O$), nickel(II) nitrate hexahydrate ($Ni(NO_3)_2{\cdot}6H_2O$), lithium nitrate ($LiNO_3$), and sucrose ($C_{12}H_{22}O_{11}$) [31]. First, stoichiometric amounts of source materials were dissolved in deionized water and continuously stirred at 80–90 °C on a hot plate. The molar ratio of source materials/sucrose was adjusted to 4:1. As the solvent evaporated, the mixed solution tuned into a viscous gel. The gel was fired at 400 °C for 1 h and a vigorous decomposition process occurred resulting in an ash-like powder. The decomposed powder was ground and the pelletized powder was heated at 850 °C for 12 h in air. It was then quenched to room temperature. To coat [Li,La]-TiO_3 on the surface of the $Li[Ni_{0.35}Co_{0.3}Mn_{0.35}]O_2$ powder, lithium nitrate ($LiNO_3$), lanthanum(II) nitrate hexahydrate ($La(NO_3)_3{\cdot}6H_2O$), and titanium(IV) butoxide ($Ti(O\text{-}C_4H_9)O_4$) were dissolved in ethanol, followed by continuous stirring for 1 h. The amount of $[Li,La]TiO_3$ was 1–5 wt% of the $Li[Ni_{0.35}Co_{0.3}Mn_{0.35}]O_2$ powder. Subsequently, NH_4OH solution was added to the solution to adjust the pH to 10. $Li[Ni_{0.35}Co_{0.3}Mn_{0.35}]O_2$ was then added to the coating solution, which was and mixed thoroughly for 4 h at room temperature. The slurry containing $Li[Li_{0.2}Ni_{0.2}Mn_{0.6}]O_2$ powders was transferred to a Teflon-sealed stainless steel autoclave and sealed tightly. Thermal treatment was carried out at 80 °C for 10 h in autogenous pressure. The product was then dried at 110 °C to remove residual water and subsequently calcined at 400 or 700 °C for 5 h. Finally, $[Li,La]TiO_3$-coated $Li[Ni_{0.35}Co_{0.3}Mn_{0.35}]O_2$ powders were obtained.

Cathodes for electrochemical evaluation were made from an active material, Super-P carbon black (Timcal Graphite & Carbon), and a polyvinylidene fluoride binder (Sigma–Aldrich) in *N*-methyl-2-pyrrolidone solvent at a weight ratio of 80:12:8, respectively. A ball milling process was carried out for 24 h to thoroughly mix the viscous slurry, which was then coated on an aluminum foil and dried at 100 °C overnight in a vacuum oven. A CR2032 type coin cell then was assembled using the prepared cathode, lithium foil (Foote Mineral Co.) employed as the anode, a polypropylene separator (Celgard Inc.), and electrolyte (1 M $LiPF_6$ dissolved in an equal-volume mixture of ethylene carbonate and dimethyl carbonate) in a glove box filled with Ar gas. Galvanostatic charge/discharge tests were performed using a cycler (Wonatech System) in a voltage range of 4.5–2.5 V between 40 and 600 mAg^{-1}. And investigation of the redox reaction occurring during the cycling process was examined 5 times by cyclic voltammetry on a potentio stat (Solatron Multistate 1480) at a scan rate of 0.1 mVs^{-1} between 2.5 and 4.5 V. For electrochemical impedance spectroscopy, a frequency response analyzer (Solartron 1260 in conjunction with a Solatron 1287 electrochemical interface) was used. Impedance measurements were examined by applying ac voltage of 10 mV over a frequency range from 0.1 to 1 MHz.

X-ray diffraction patterns (XRD, RINT2000, Rigaku) were obtained using Cu Kα radiation in a 2θ range of 15°–70°. The microstructure of the particles was examined by a transmission electron microscope (TEM, JEM3010, 300 kV, JEOL). Information on the surface composition was gathered examined by X-ray photoelectron spectroscopy (XPS, VG Scientific). For preparing differential scanning calorimetry (TA Instrument Q-10) samples of the cathodes, coin cells were charged to 4.5 V at 40 $mAhg^{-1}$, and then held them at that voltage for 10 h. The cells were disassembled to achieve charged cathodes. Sealed samples for differential scanning calorimetry tests were heated to 300 °C, and the scan rate was 3 °C/min.

3 Results and discussion

The XRD patterns and Miller indices of the pristine powder and various amounts (1–5 wt%) of $[Li,La]TiO_3$-coated $Li[Ni_{0.35}Co_{0.3}Mn_{0.35}]O_2$ samples are shown in Fig. 1. The XRD patterns of the pristine and coated materials exhibited patterns corresponding to a layered α-$NaFeO_2$ type structure (space group, R-3m). The XRD patterns appeared to be

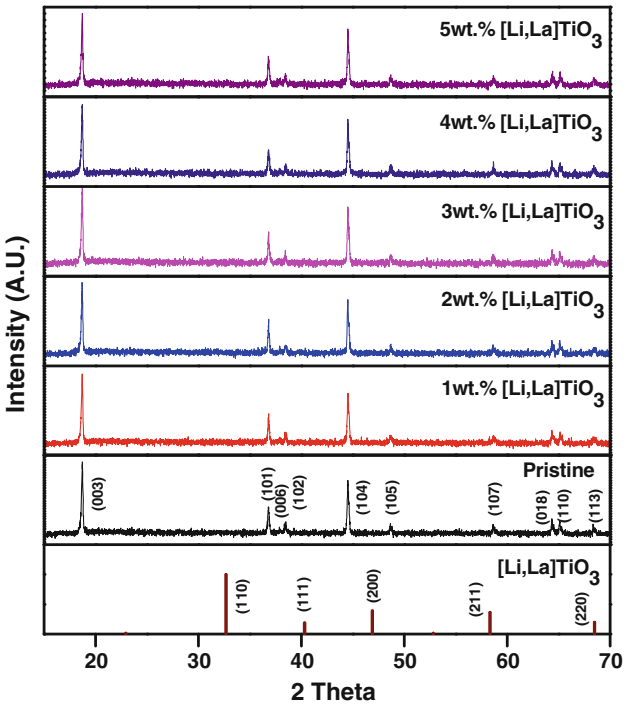

Fig. 1 XRD patterns of the layered oxide $Li[Ni_{0.35}Co_{0.3}Mn_{0.35}]O_2$ before and after surface coating with various amounts (0–5 wt%) of $[Li,La]TiO_3$ followed by annealing at 400 °C

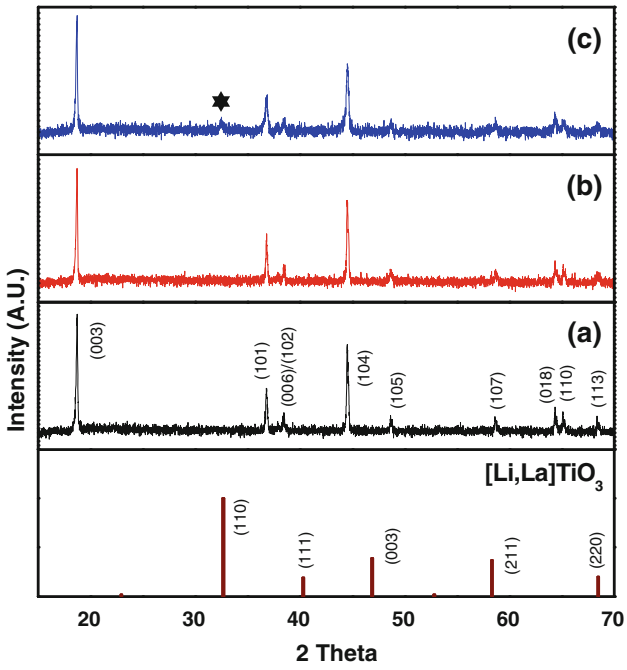

Fig. 2 XRD patterns of the layered oxide $Li[Ni_{0.35}Co_{0.3}Mn_{0.35}]O_2$ before and after surface coating with 10 wt% $[Li,La]TiO_3$ followed by annealing at 400 and 700 °C: (*a*) the pristine, (*b*) after surface coating followed by annealing at 400 °C, (*c*) after surface coating followed by annealing at 700 °C

almost identical for all of the materials, and secondary phase peaks for the coating materials were not detected. All of the samples showed good layer hexagonal ordering, regardless of the $[Li,La]TiO_3$ content up to 5 wt%. Splitting of (018)/(110) is well known to indicate a high degree of crystallinity and good layered hexagonal ordering [16]. The absence of peaks corresponding to lithium lanthanum titanate in Fig. 1 suggests two possibilities: that secondary phase peaks for the coating material were not found because the amount of coating material on the layered oxide was too small to be detected, or that the temperature (400 °C) during the coating process was too low for crystallization of the coating material. Because XRD patterns of lithium lanthanum titanate were detected in the coated powder when the heating temperature in the coating process was over 700 °C, as shown in Fig. 2, the coating layers were inferred to be present in the form of an amorphous phase. On the other hand, XRD data for $Li[Ni_{0.35}Co_{0.3}Mn_{0.35}]O_2$ at 700 °C that had been surface modified with 2 wt% lithium lanthanum titanate did not show any peak corresponding to a perovskite-type structure. This confirmed that a very small amount of the coating layer was present in the form of an amorphous oxide. The XRD patterns of coated particles are known to conform to the symmetry of the core materials irrespective of the coating material method because the coating material is present as a thin film, possibly as a mixed oxide formed by intercalation of the coating oxide with the core material [12, 13, 16, 17, 19, 20]. Transmission electron microscopy (TEM) was used to investigate the surface shape of the pristine and surface-modified particles in detail. Figure 3 shows TEM images of the surface morphology for the pristine and coated $Li[Ni_{0.35}Co_{0.3}Mn_{0.35}]O_2$ powders. The pristine sample exhibited a smooth surface with no other layer on the surface; in contrast, the surface of the coated powder showed a coating layer by heteroelements. It appears that the formed coating layer is porous relative to the core material, as shown in the contrasts for the image in Fig. 3b. The inset of Fig. 3b shows two types of selected area diffraction (SAD) spots of the coated material. The SAD spot corresponding to the coating layer demonstrates an amorphous phase, whereas the SAD spot of the core material indicates that the active material is a single crystal with hexagonal ordering. The coating material was confirmed to be in an amorphous phase on the layered cathode materials through XRD and TEM analyses. It is expected that the amorphous layer obtained in this experiment would facilitate the transport of Li ions across the surface owing to its open structure compared to a crystalline layer; the coating layer appears to be porous in comparison with the core material regardless of the composition of the coating material.

Figure 4 shows the XPS analysis data for the samples before and after surface modification with lithium lanthanum titanate. XPS is extensively used in characterizing the

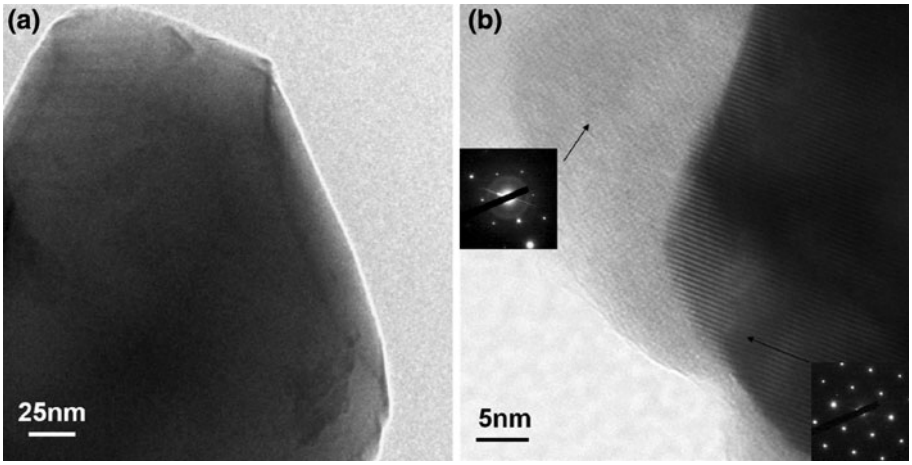

Fig. 3 TEM images of the **a** pristine, **b** 2 wt% [Li,La]TiO_3-coated $Li[Ni_{0.35}Co_{0.3}Mn_{0.35}]O_2$. *Inset* parts are SAD spot of checked point with arrows on the **b** image

surface composition of cathode materials [20]. The binding energies are listed in Table 1; those of the $Mn(2p_{3/2})$, $Co(2p_{3/2})$, and $Ni(2p_{3/2})$ peaks are close to the values for Mn^{4+}, Co^{+3}, and Ni^{2+}, respectively, regardless of surface modification [9, 32]. This means that the oxidation states for Mn, Co, and Ni in this study were 4+, 3+, and 2+, respectively. It is noted that no La or Ti peaks attributable to the surface coating layers were found in the pristine sample, while apparent La and Ti peaks were observed in the coated material. Thus, La and Ti elements existed on the surface of the layered cathode material as a surface-modifying material. This was also supported by decreases in the intensities of $Mn(2p_{3/2})$, $Co(2p_{3/2})$, and $Ni(2p_{3/2})$ in the coated sample as compared to the pristine sample, due to decreases in the Mn, Co, and Ni content on the surface. These results agree well with the TEM analysis results in Fig. 3 showing distinct amorphous coating layers. Figure 4 presents decreases in the intensities of $La(3d_{5/2})$ and $Ti(2p_{3/2})$ upon increasing the annealing temperature to 700 °C as compared to the intensities for the sample annealed at 400 °C. The decreased intensities are due to enhanced diffusion of the La and Ti elements into the active material, and decreased La and Ti content on the surface [32].

Figure 5 compares the discharge capacity and cyclic performance of the pristine and [Li,La]TiO_3-coated $Li[Ni_{0.35}Co_{0.3}Mn_{0.35}]O_2$ electrodes at various current densities for voltages of 2.5–4.5 V. In experiments investigating the effects of the coating on the capacity, cyclic performance, and rate capability, the results showed marked improvement in the electrochemical properties for the coated samples as compared to the pristine samples in terms of cycle life performance, as shown in Fig. 5. At a current density of 40 mA g^{-1}, the initial capacity and capacity retention of the electrode containing 2 wt% coating material were 189 $mAhg^{-1}$ and 79%, respectively; these were the highest initial capacity and capacity retention measured among the samples. However, the differences in the initial capacity and capacity retention during cycling between the pristine and various coated (1–5 wt%) samples were not crucial. As shown in Fig. 5b, the 2 wt% coated material had a 147 $mAhg^{-1}$ initial capacity and 89% capacity retention, while the initial capacity and capacity retention of the pristine powder were 118 $mAhg^{-1}$ and 64%, respectively. The rate capability results for the pristine and coated powders, as shown in Fig. 5c, demonstrate that the 2 wt% coated powder had superior capacity and capacity retention, with values of 91 $mAhg^{-1}$ and 71%, respectively. In contrast, the pristine powder showed 75 $mAhg^{-1}$ initial capacity and 38% capacity retention. The 1 and 3 wt% coated powders exhibited inferior properties compared to those of the pristine powder. The electrochemical behavior for the 1 and 3 wt% coated samples indicates that the amount of the coating layer should be carefully chosen. The notable improvement in the cyclic performance for the $Li[Ni_{0.35}Co_{0.3}Mn_{0.35}]O_2$ samples may have been achieved by introducing the 2 wt% [Li,La]TiO_3 coating material at all of the low and high current densities.

As shown in Fig. 6, the electrochemical properties of pristine $Li[Ni_{0.35}Co_{0.3}Mn_{0.35}]O_2$ and that containing 2 wt% coating material were characterized in order to investigate the effect of the annealing temperature on the coating. The sample annealed at 700 °C showed the lowest initial capacity at 40, 200, and 600 mAg^{-1}, which correspond to 159, 72, and 65 $mAhg^{-1}$, respectively. However, at a high rate density (600 mAg^{-1}), the electrode had a higher discharge capacity than the pristine powder. The coated material annealed at 400 °C showed the best capacity retention at all current states in the experiments, and the effects of the coating on the rate capability were manifested regardless of the annealing temperature. The enhanced cycle life performance due to surface modification is similar to results reported previously [12–20]. In the [Li,La]TiO_3 system, the composition, structure, and phase are significant factors when considering ionic and electronic conductivities [22–25]. The phase of the lithium

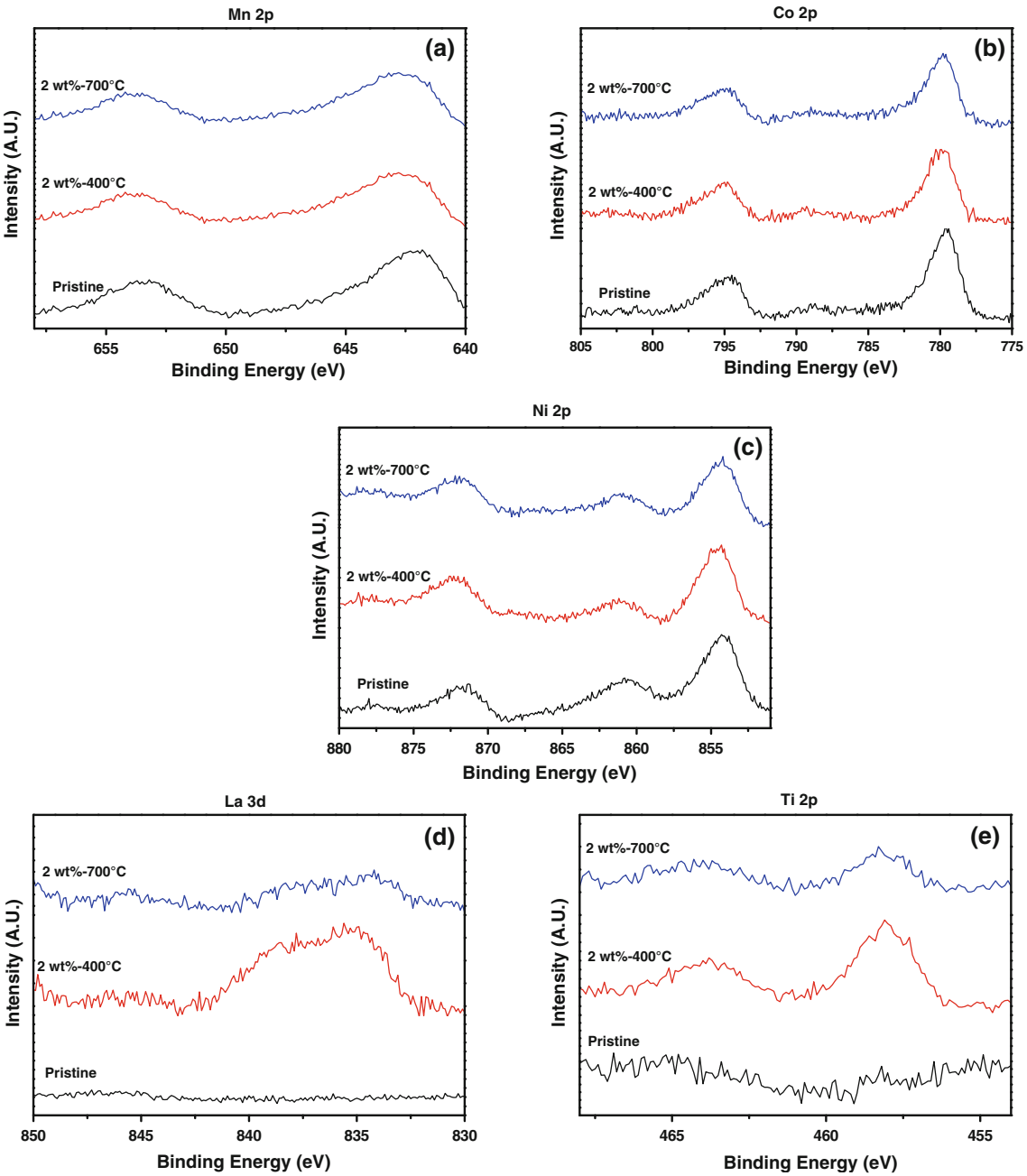

Fig. 4 XPS spectra of pristine and [Li,La]TiO_3-coated $Li[Ni_{0.35}Co_{0.3}Mn_{0.35}]O_2$ Particles: **a** Mn, **b** Co, **c** Ni, **d** La, **e** Ti

Table 1 Binding energies (eV) of elements in pristine and [Li,La]-TiO_3-coated $Li[Ni_{0.35}Co_{0.3}Mn_{0.35}]O_2$

Sample	Mn 2p	Co 2p	Ni 2p	La 3d	Ti 2p
Pristine	642.0	779.5	854.2	–	–
2 wt%-400 °C	642.4	779.9	854.6	834.5	458.1
2 wt%-700 °C	642.3	779./8	854.3	834.3	458.2

lanthanum titanate was investigated as a function of temperature using XRD and TEM; the powders annealed at 400 or 700 °C were confirmed to have amorphous and crystalline phases, respectively, with a perovskite structure. Higher temperature was shown to facilitate the diffusion of elements in the coating material; this phenomenon caused loss of the coating layer, according to the XPS analysis results of Fig. 4. Therefore, the difference in the capacity retention between the coated samples, as shown in Fig. 6, may be due to the phase of the coating material, in agreement with the earlier TEM analysis, as well as the decreased La and Ti contents on the surface due to enhanced diffusion of the La and Ti elements into the layered oxide.

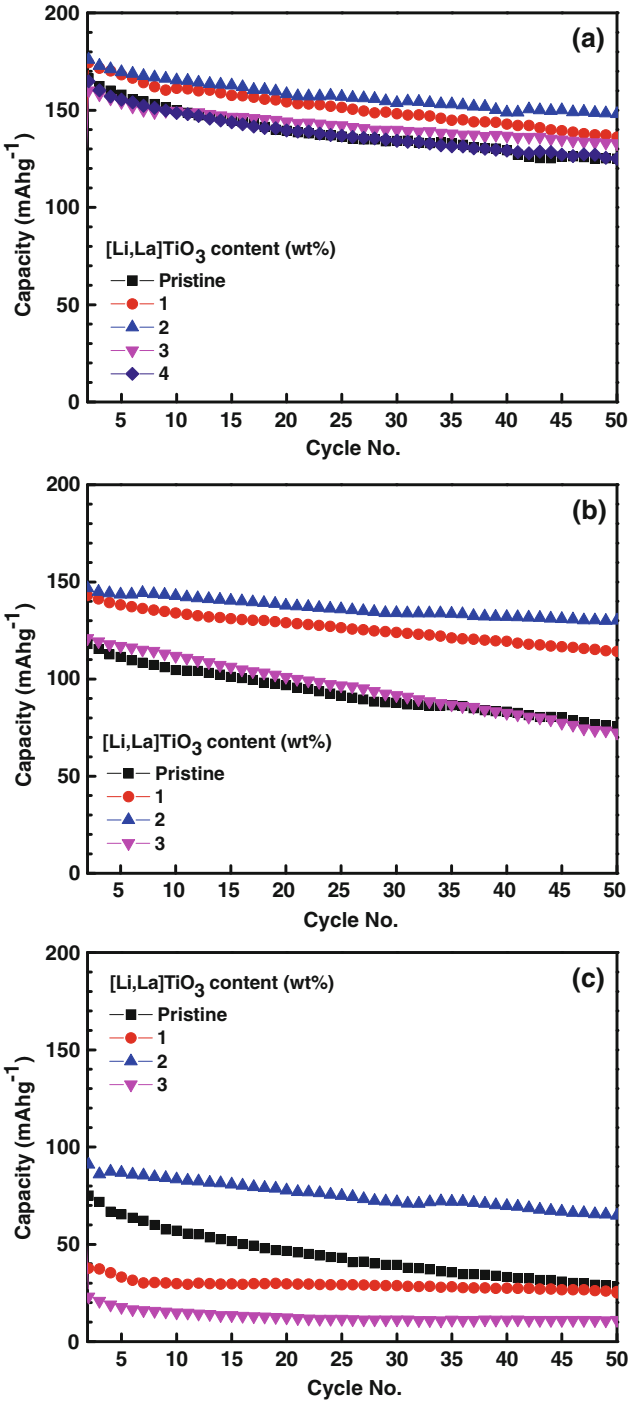

Fig. 5 Cycle performances of the layered oxide $Li[Ni_{0.35}Co_{0.3}Mn_{0.35}]O_2$ before and after surface coating with various amounts (1–5 wt%) of $[Li,La]TiO_3$ followed by annealing at 400 °C at various current densities: **a** 40 mAg^{-1}. **b** 200 mAg^{-1}, **c** 600 mAg^{-1}

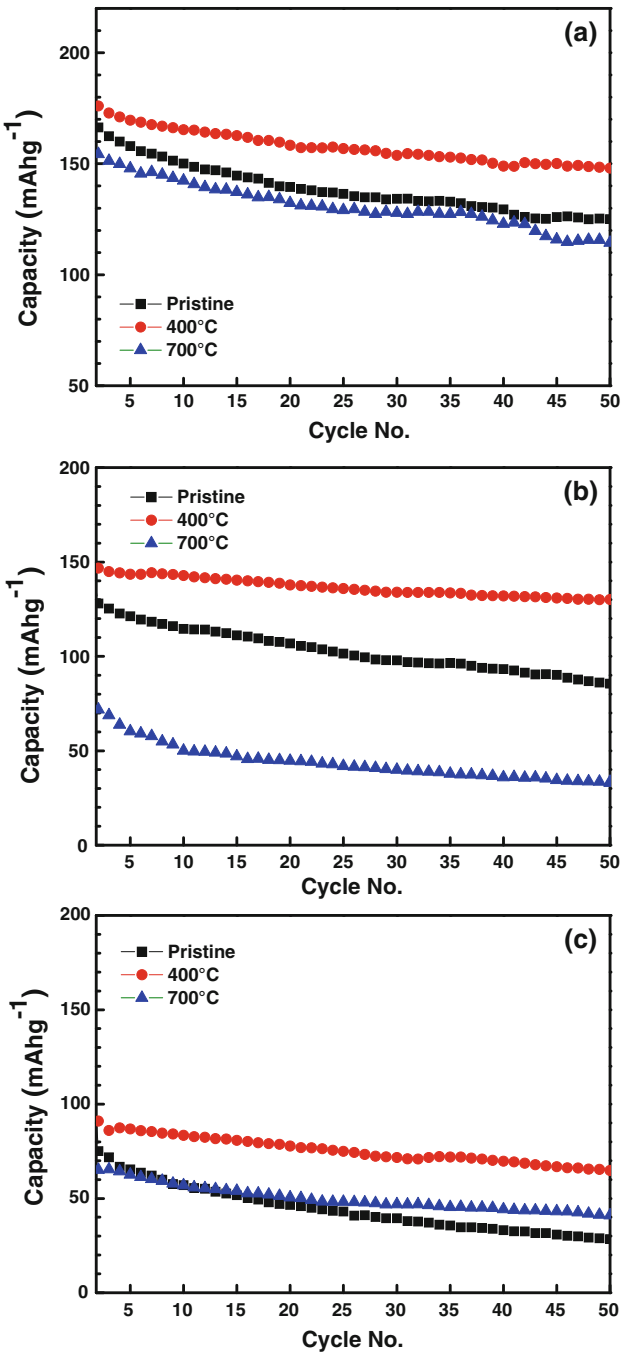

Fig. 6 Cycle performances of the layered oxide $Li[Ni_{0.35}Co_{0.3}Mn_{0.35}]O_2$ before and after surface coating with 2 wt% of $[Li,La]TiO_3$ followed by annealing at 400 or 700 °C at various current densities: **a** 40 mAg^{-1}, **b** 200 mAg^{-1}, **c** 600 mAg^{-1}

Electrochemical impedance spectroscopy was performed to elucidate the electrochemical characteristics of the pristine and $[Li,La]TiO_3$-coated $Li[Ni_{0.35}Co_{0.3}Mn_{0.35}]O_2$ electrodes and to clarify the coating effects. Similar studies have also been reported for many positive electrode materials, such as ZrO_2-coated $Li[Li_{1/6}Mn_{1/6}Co_{1/6}Ni_{1/6}]O_2$ [16], $AlPO_4$-coated $Li[Li_{0.2}Mn_{0.54}Co_{0.13}Ni_{0.13}]O_2$ [32], and $Li[Mn_{1/3}Co_{1/3}Ni_{1/3}]O_2$ [8]. Figure 7a presents the electrochemical impedance spectroscopy results of the pristine sample and samples with various amounts (1–4 wt%) of $[Li,La]TiO_3$ coating. The

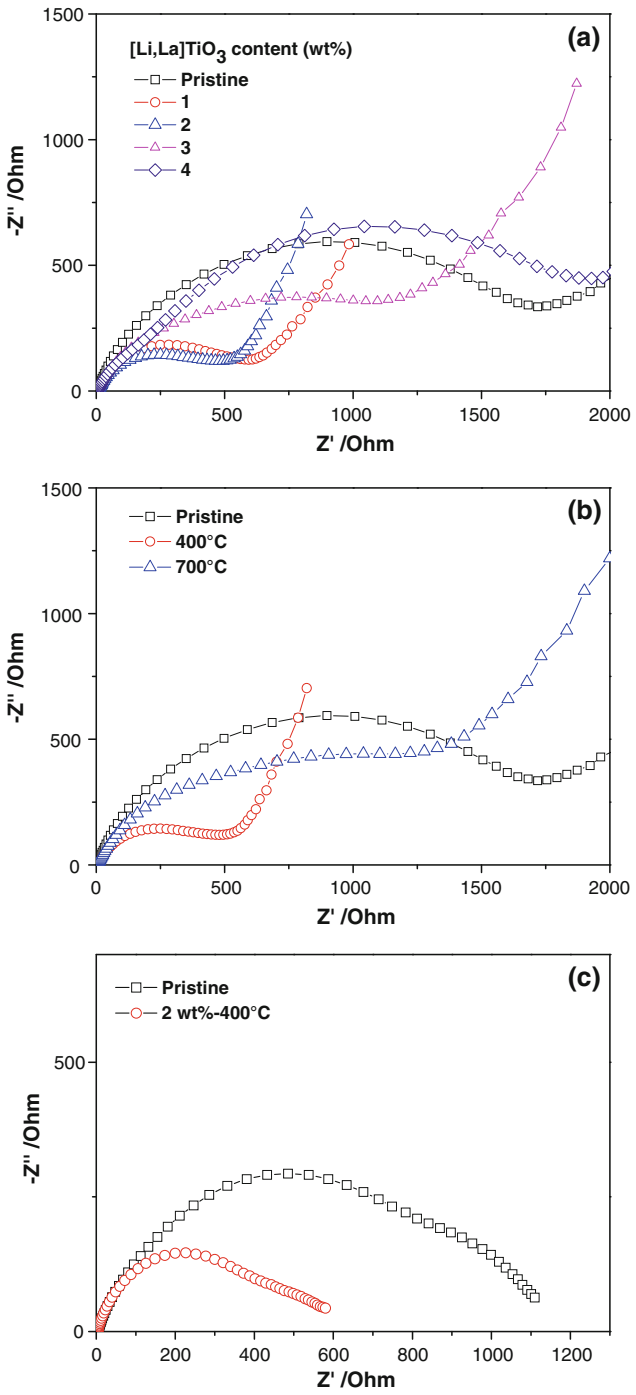

Fig. 7 Nyquist plots of the layered oxide $Li[Ni_{0.35}Co_{0.3}Mn_{0.35}]O_2$ before and after surface coating **a** with various amounts (1–5 wt%) of $[Li,La]TiO_3$ followed by annealing at 400 °C, **b** with 2 wt% $[Li,La]TiO_3$ followed by annealing at 400 or 700 °C, **c** the pristine, and 2 wt% $[Li,La]TiO_3$-coated $Li[Ni_{0.35}Co_{0.3}Mn_{0.35}]O_2$ electrodes after 50 cycles at 600 mAg^{-1}

2 wt% $[Li,La]TiO_3$-coated $Li[Ni_{0.35}Co_{0.3}Mn_{0.35}]O_2$ sample showed the smallest impedance, and the impedance for the 1 wt% coated sample was slightly larger. The sample with 3 wt% $[Li,La]TiO_3$ had a noticeably larger impedance than the above two samples, and the impedance was larger than that of the pristine electrode when the coating material reached 4 wt%, as indicated by the semicircles in Fig. 7a. These observations reveal that surface coating of up to 3 wt% $[Li,La]TiO_3$ lowers the impedance of the $Li[Ni_{0.35}Co_{0.3}Mn_{0.35}]O_2$ sample, and surface modification with >3 wt% $[Li,La]TiO_3$ leads to a noticeable increase in the impedance relative to that of the pristine electrode. As shown in Figs. 5b and 7a, samples with enhanced capacity retention show smaller semicircles. In Fig. 5c, the 1 wt% coated sample does not exhibit an improved discharge profile, although the sample had the second smallest impedance. This suggests that a 1 wt% coating of $[Li,La]TiO_3$ is not adequate to obtain sufficient coating effects. Thus, a coating in excess of 1 wt% is needed to enhance the rate capability of $Li[Ni_{0.35}Co_{0.3}Mn_{0.35}]O_2$. Therefore, surface coating with 2 wt% $[Li,La]TiO_3$ is the optimal condition for $Li[Ni_{0.35}Co_{0.3}Mn_{0.35}]O_2$: it shows the smallest impedance and delivers a sufficient coating effect. Figure 7b shows that the coated samples had smaller impedances than the pristine electrode irrespective of the annealing temperature; the sample annealed at 400 °C had the smallest impedance. However, the discharge capacity and cyclic performance of the electrode annealed at 700 °C were not better that those of the pristine electrode. The electrochemical properties for the electrode annealed at 700 °C are likely due to enhanced diffusion of La and Ti element into the active material, which decreases the La and Ti contents on the surface, as shown by the XPS analysis. In general, a high frequency semicircle is related to a passivating surface film, a so called solid electrolyte interface, and an intermediate frequency semicircle is attributed to charge transfer resistance in the electrode/electrolyte interface [16]. In Fig. 7c, the fitted values of the high frequency and intermediate frequency semicircles are 750 and 435 Ω, respectively, in the pristine sample and 429 and 157 Ω, respectively, in the $[Li,La]TiO_3$-coated sample. The sizes of all high and intermediate frequency semicircles for the pristine sample were much larger than those of the $[Li,La]TiO_3$-coated samples. Therefore, impedance growth by the solid electrolyte interface is suppressed by the $[Li,La]TiO_3$ coating layer during cycling, and the $[Li,La]TiO_3$ coating layer prevents electrode/electrolyte interfacial degradation stemming from corrosion or dissolution of cathode material into the electrolyte [29].

Figure 8 presents the cyclic voltammograms of the pristine and 2 wt% $[Li,La]TiO_3$-coated $Li[Ni_{0.35}Co_{0.3}Mn_{0.35}]O_2$ samples. This figure shows only one major peak, corresponding to the redox-reaction peak in the cyclic voltammograms, despite a difference between the 5-times charge and discharge performances. It is known that the major peak has been attributed to the redox reaction of Ni^{2+}/Ni^{3+}, Ni^{2+}/Ni^{4+}, and/or Co^{3+}/Co^{4+} [9]. The analysis of the cyclic voltammogram in Fig. 8 indicates that the major peak is

caused by Ni^{2+} and Co^{3+}, which confirms that the Ni and Co states are 2+ and 3+, respectively, as shown in Fig. 4. Thus, [Li,La]TiO_3 was confirmed to be inactive with respect to the intercalation and deintercalation of lithium ions and acts only as a surface modification material for the tested voltages. No considerable change in the position or intensity of the peak was observed during cycling. This indicates that the initial layered crystal structure was maintained, with no phase transitions or unexpected side reactions. As shown in Fig. 8, compared to the pristine sample, the major oxidation peak of the coated sample shifted to a lower voltage, and the reduction peak shifted to a higher voltage. This means that the polarization of the $Li[Ni_{0.35}Co_{0.3}Mn_{0.35}]O_2$ sample decreased because of the [Li,La]TiO_3 coating layer. This decrease in the polarization of the samples is likely due to a decrease in the cell resistance as a result of the coating effects. This was confirmed by the electrochemical impedance spectroscopy analysis, which examined the decrease in impedance of the coated electrode compared with that of the pristine sample.

Differential scanning calorimetry was performed to compare the thermal stability of the $Li[Ni_{0.35}Co_{0.3}Mn_{0.35}]O_2$ electrodes before and after 2 wt% [Li,La]TiO_3 coating at a charging state of 4.5 V, and the results are shown in Fig. 9. The exothermic peak was attributed to the amount of heat generated due to oxygen generation from the decomposed cathode oxides and reactions with the electrolyte. The exothermic peak of the pristine sample was generated at about 226 °C, while the coated sample showed better thermal stability, with an exothermic temperature of about 240 °C. The higher exothermic temperature of the coated particles indicates that the amount of oxygen generated from decomposition of the layered oxides was much lower than that of the uncoated cathode oxide.

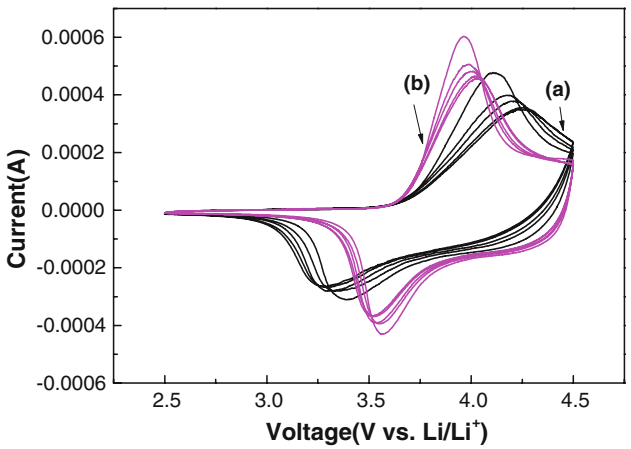

Fig. 8 Cyclic voltammograms of the (*a*) pristine, (*b*) 2 wt% [Li,La]TiO_3-coated $Li[Ni_{0.35}Co_{0.3}Mn_{0.35}]O_2$

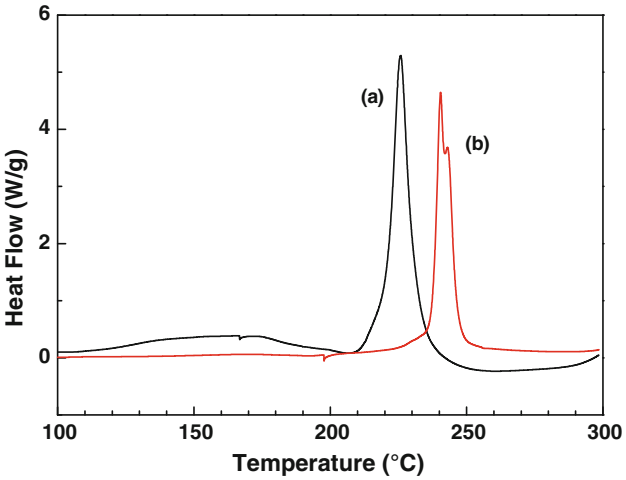

Fig. 9 Differential scanning calorimetry thermograms of the pristine, 2 wt% [Li,La]TiO_3-coated $Li[Ni_{0.35}Co_{0.3}Mn_{0.35}]O_2$ electrodes after charged at 4.5 V

4 Conclusion

A novel coating material, [Li,La]TiO_3, was introduced as a coating powder for an $Li[Ni_{0.35}Co_{0.3}Mn_{0.35}]O_2$ cathode, and the coating effects were examined. [Li,La]TiO_3 coated $Li[Ni_{0.35}Co_{0.3}Mn_{0.35}]O_2$ cathode materials exhibited improved cycle life performance and thermal stability. The morphology and composition of the coating layers were investigated using TEM and XPS. The phase and content of the coating material depended on the heating temperature. XPS data show decreased La and Ti content when the annealing temperature was increased to 700 °C, compared to when the sample was annealed at 400 °C. The optimal coating layer on the surface of the cathode material was confirmed to be an amorphous phase annealed at 400 °C. Electrochemical impedance spectroscopy was used to identify coating effects and the relation between the impedance and electrochemical properties. Coating layers were confirmed to suppress the solid electrolyte interface during cycling by electrochemical impedance spectroscopy. The improved thermal stability achieved by the coating material was characterized by differential scanning calorimetry.

Acknowledgment This research was supported by the Converging Research Center Program through the Ministry of Education, Science and Technology (2010K001089).

References

1. Ozawa K (1994) Solid State Ionics 69:212
2. Cheng C, Tan L, Hu A, Liu H, Huang X (2010) J Alloys Compd 506:888
3. Riley LA, Atta SV, Cavanagh AS, Yan Y, George SM, Ping L, Dillon AC, Lee SH (2011) J Appl Electrochem 196:3317

4. Choi J, Manthiram A (2005) Solid State Ionics 176:2251
5. Kim KM, Lee SH, Kim S, Lee YG (2009) J Appl Electrochem 39:1487
6. Wu F, Lu H, Su Y, Li N, Bao L, Chen S (2010) J Appl Electrochem 40:783
7. Song MY, Kwon SN, Yoon SD, Mumm DR (2009) J Appl Electrochem 39:807
8. Reale P, Privitera D, Panero S, Scrosati B (2007) Solid State Ionics 178:1390
9. Tang A, Huang K (2005) Mater Sci Eng B 122:115
10. Zhu C, Yang C, Yang WD, Wu MS, Ysai HM, Hsieh CY, Fang HL (2010) J Appl Electrochem 40:1665
11. Mantia FL, Rosciano F, Tran N, Novak P (2009) J Electrochem Soc 156:A823
12. Li C, Zhang HP, Fu LJ, Liu H, Wu YP, Rahm E, Holze R, Wu HQ (2006) Electrochim Acta 51:3872
13. Fu LJ, Liu H, Li C, Wu YP, Rahm E, Holze R, Wu HQ (2006) Solid State Sci 8:113
14. Li H, Wang Z, Chen L, Huang X (2009) Adv Mater 21:1
15. Ryu KS, Lee SH, Koo BK, Lee JW, Kim KM, Park YJ (2008) J Appl Electrochem 38:1385
16. Kim GY, Park YJ, Jung KH, Yang DJ, Lee JW, Kim HG (2008) J Appl Electrochem 38:1477
17. Fey GTK, Lu CZ, Huang JD, Kumar TP, Chang YC (2005) J Power Sources 146:65
18. Kweon HJ, Kim SJ, Park DG (2000) J Power Sources 88:255
19. Cho J, Kim TJ, Kim J, Noh M, Park B (2004) J Electrochem Soc 151:A1899
20. Hu GR, Deng XR, Peng ZD, Du K (2008) Electrochim Acta 53:2567
21. Kim YJ, Cho J, Kim TJ, Park B (2003) J Electrochem Soc 150:A1723
22. Inaguma Y, Matsui Y, Shan YJ, Itoh M, Nakamura T (1995) Solid State Ionics 79:91
23. Oguni M, Inaguma Y, Itoh M, Nakamura T (1994) Solid State Commun 91:627
24. Inaguma Y, Liquan C, Itoh M, Nakamura T, Uchidam T, Ikuta H, Wakihara M (1993) Solid State Commun 86:689
25. Inaguma Y, Chen L, Itoh M, Nakamura T (1994) Solid State Ionics 70:196
26. He LX, Yoo HI (2003) Electrochim Acta 48:1357
27. Maruyama Y, Ogawa H, Kamimura M, Ono S (2008) Ionics 14:357
28. Inoue N, Zou Y (2005) Solid State Ionics 176:2341
29. Myung ST, Izumi K, Komaba S, Yashiro H, Bang HJ, Sun YK, Kumagai N (2007) J Phys Chem C 111:4061
30. Lee H, Kim Y, Hong YS, Kim Y, Kim MG, Shin NS, Cho J (2006) J Electrochem Soc 153:A781
31. Yi SB, Chung HT, Kim HG (2007) Electrochem Commun 9:591
32. Wu Y, Murugan AV, Manthiram A (2008) J Electrochem Soc 155:A635